Tsunami hazard in Caribbean Coast of Honduras due to Large Earthquakes Occurred along the Cayman Trough at the Northwest boundary of Caribbean plate.

Yuichiro Tanioka[1)], Amilcar Geovanny Cabrera[2)], Greyving Jose Arguello[2)],
and Yusuke Yamanaka[3)]

1) Institute of Seismology and Volcanology, Faculty of Science, Hokkaido University, N10W8, Kita-ku, Sapporo, Japan, 060-0810
2) Nicaraguan Institute of Territorial Studies, Managua, Nicaragua.
3) Department of Civil Engineering, The University of Tokyo, Tokyo 113-8656, Japan

(Revised parts are shown in red.)

Abstract

In 2018, a large earthquake (Mw7.6) occurred in the Swan Island Fault zone at the northwest boundary of the Caribbean plate. This earthquake generated only a small tsunami of 20 cm. However, Puerto Cortes in Honduras is located close to the Swan Island Fault zone. Evaluation of tsunami hazard at Puerto Cortes due to large earthquakes along the fault zone is important. We first estimated the fault parameters of the 2018 Swan Island earthquake using W-phase inversion technique. Then, the moment magnitude of 7.6, the fault length of 134 km, the fault width of 24 km, and the slip amount of 5.1 m were estimated. In addition to those estimates, a small fault dimension of the earthquake, 40 km × 20 km, with a slip amount of 20.8 m was considered. Those two fault models were used to compute tsunami inundation at Puerto Cortes. The tsunami computed from the small fault inundated a large area in Puerto Cortes including the port area. The effect of co-seismic horizontal displacement of ocean floor also enhanced the tsunami inundation there. Those results indicate that preparation for future tsunami hazard in Puerto Cortes is important although no significant tsunami was generated historically.

Key words: Tsunami hazard; Puerto Cortes in Honduras; The 2018 Swan Island earthquake.

1. Introduction

On 9th of January in 2018, a large earthquake (Mw7.6) occurred in the Swan Island Fault zone at the northwestern boundary of the Caribbean plate (Figure 1). The location and mechanism of the earthquake from the Global CMT catalog show a left-lateral strike-slip fault motion along the Swan Island fault zone. The tsunami warning was issued from the Pacific Tsunami Warning Center immediately after the earthquake. Only small tsunami was generated by the earthquake

and was observed at George Town in Cayman Islands, United Kingdom. The observed amplitude of the tsunami was about 20 cm.

The 2010 large Haiti earthquake (Mw7.0) generated tsunamis along the coast of Haiti in Caribbean Sea (Fritz et al., 2013). Historically, several large earthquakes have occurred along the Swan Island fault zone (Figure 1). In 1976, the Guatemala large earthquake (Ms7.5) occurred along the Motagua fault which is located at the western end of the Swan Island fault zone (Plafker, 1977). The surface rupture was extended about 230 km with a left-lateral displacement. The strong shaking caused more than 23,000 casualties, the most destructive earthquake in Guatemala since 1917. Because the earthquake occurred inland, the tsunami was not generated. In 1999, the Guatemala earthquake (Mw 6.7) occurred beneath the Caribbean coast of Guatemala with a left-lateral fault motion. The strong motion caused one casualty and destroyed several houses in Guatemala. In 2009, the off-Honduras earthquake (Mw7.3) occurred along the Swan Island fault zone in Gulf of Honduras (Figure 1). The strong shaking in northern Honduras caused 7 casualties and destroyed 130 buildings (https://earthquake.usgs.gov/earthquakes/eventpage/usp000gxkj/impact).

Although there were no damages reported by tsunamis generated by those historical large earthquakes, the concern of tsunami risk along the northern coast of Honduras has been increased after the 2018 large Swan Island earthquake. Especially, evaluation of the tsunami risk at Puerto Cortes in Honduras, one of the largest seaports in Central America, is an important issue because Puerto Cortes is located very close to the Swan Island fault zone (Figure 1). Also, in 2016, the Central American Tsunami Advisory Center (CATAC) was started to establish at the Nicaraguan Institute of Territorial Studies with Japanese cooperation (Strauch et al., 2018). This center should be completed in 2019. Evaluation of tsunami hazard along the coast in Central America is also one of important tasks in the CATAC.

In this study, at first, the source model of the 2018 large Swan Island earthquake is determined by using the W-phase inversion (Kanamori and Rivera, 2008) and the scaling relationship (Blaser

et al., 2010). Then, the tsunami hazard at Puerto Cortes in the northern coast of Honduras is evaluated from realistic fault models based on the fault models of the 2018 large Swan Island earthquake. Finally, the tsunami risk at Puerto Cortes in Honduras is discussed.

2. Data

Low-frequency broadband seismic records from the database at the German Research Center for Geosciences (GRCG or GFZ) catalog were downloaded. The vertical components of 49 stations located at epicentral distance less than 90 degrees are used for the W-phase inversion. The General Bathymetry Chart of the Oceans (GEBCO) dataset of 30 arcseconds grid spacing, the nautical chart (#28170) of Puerto Cortes (Gulf of Honduras), and the topography data, Shuttle Radar Topography Mission (SRTM) with a resolution of 1 arcseconds, are used for the tsunami inundation simulation.

3. Method

3.1 Estimation of Fault model

The W phase, a distinct long-period (100–1000 s) phase arrives before the S phase and can be used for rapid and robust determination of great earthquake source parameters (Kanamori and Rivera 2008; Duputel et al. 2011). This W-phase inversion algorithm is used to estimate the magnitudes, the centroid locations, and the mechanisms of the 2018 Swan Island earthquake (Mw7.6). Time domain deconvolution is used to retrieve displacement waveforms from the broadband seismograms. Then, they are bandpass filtered between 0.00167 and 0.005 Hz using fourth order of Butterworth filter. The time window (in seconds) used in the inversion is set between P wave arrival and that plus 15 times the distance (degree) between the epicenter and the station.

Scaling relationships are used to estimate the length and width of the fault model from the estimated moment magnitude by the W-phase inversion. Blaser et al. (2010) determined the empirical relationship between the fault length, L (km), and moment magnitude, Mw, as shown in Equation (1), and the relationship between the fault width, W (km), and moment magnitude, Mw, as shown in Equation (2) for large oceanic strike-slip earthquakes in the world.

$$\log L = -2.56 + 0.62Mw \quad (1)$$

$$\log W = -0.66 + 0.27Mw \quad (2)$$

A slip amount, D (m), is calculated from Equation (3):

$$D = \frac{M_0}{\mu LW} \text{ , where } M_0 = 10^{1.5M_w+9.1} \quad (3)$$

where M_0 (Nm) is the seismic moment, L is the fault length in m, W is the fault width in m, and μ is a rigidity that is assumed to be $1.7 \times 10^{10}\ N/m^2$, which is the smallest for shallow earthquakes in the crust. The center of the fault is located at the centroid of the W-phase inversion.

3.2. Tsunami Numerical Simulation

The vertical ocean bottom deformation due to an earthquake is computed from the fault model using the equations of Okada (1985). Then, the vertical ocean surface deformation due to the co-seismic horizontal displacement of ocean bottom (Tanioka and Satake, 2006) is added to the co-seismic vertical deformation. This vertical deformation is used as the tsunami initial surface deformation. The tsunami propagation is numerically computed using the non-linear shallow water equations solved by the finite difference scheme (Goto et al. 1997). Tsunami inundation is numerically computed using a moving boundary condition (Imamura 1996). A Manning's roughness coefficient in the non-linear shallow water equations is assumed to be 0.025 $sm^{-1/3}$. Four nested grid systems are used for this tsunami simulation (Figure 2). For Region 1 (R1), the bathymetry GEBCO 30 arcseconds was resampled to make 27 arcseconds grid system. For Regions 2 and 3 (R2 and R3), it was interpolated to make 9 and 3 arcseconds grid systems, respectively. For Region 4 (R4), the nautical cart (#28170) for Puerto Cortes was digitized and

130 combined with Shuttle Radar Topography Mission (SRTM) 1 arcsecond topography data to make
131 1 arcsecond grid system. Finally, the 1 arcsecond topography data along the coast of Puerto Corte
132 are manually corrected using the topography map (Figure 3).
133
134 ## 4. Result
135
136 ### *4.1. Fault model for the 2018 Swan Island earthquake*
137 The solution of W-phase inversion gives a seismic moment of 2.85 x 10^{20} Nm (Mw 7.57), a
138 left-lateral strike-slip mechanism (strike = 254.4°, dip = 66.8°, rake = -11.1°), a centroid location
139 (longitude 83.75°W, latitude 17.46°N), a centroid depth of 11.5 km (Figure 4). The fault length
140 and width estimated from the scaling relationships, equation (1) and (2), (Blaser et al., 2010) are
141 134 km and 24 km, respectively. The slip amount is calculated to be 5.1 m using equation (3).
142 The estimated slip distribution of the 2018 Swan Island earthquake was shown in the USGS
143 earthquake catalog (https://earthquake.usgs.gov/earthquakes/eventpage/us1000c2zy/finite-fault).
144 This indicated that the slip was more concentrated near the epicenter, the fault length of about 40
145 km and the fault width of about 20 km. This may indicate that the world-wide scaling relationships
146 do not work for large earthquakes in this fault zone. Therefore, we decided to use this small fault
147 area of 40 km x 20 km for one of fault models to evaluate tsunami hazard at Puerto Cortes in
148 Honduras. The slip amount for the small fault is calculated to be 20.8 m.
149
150 ### *4.2. Tsunami inundation simulation at Puerto Cortes*
151 A long fault model of 136 km x 24 km using the scaling relationships and a small fault model
152 of 40 km x 20 km based on the slip distribution of the 2018 earthquake are used to compute
153 tsunami inundation at Puerto Cortes in Figure 3. We located these fault models off Puerto Cortes
154 along the Swan Island fault zone (Figure 4). The mechanism and the seismic moment are the same
155 as the 2018 Swan Island earthquake. The co-seismic horizonal displacement of the ocean bottom

156 (Tanioka and Satake, 1996) should be important for the tsunami generation because of the strike-
157 slip type of the fault models. Therefore, four tsunami inundations at Puerto Cortes are numerically
158 computed using two fault models with the tsunami generation due to the horizontal displacement
159 or without that.

160 In Figure 5, the tsunami initial conditions from the long fault model with the effect of the
161 horizontal displacement and without that are compared. In Figure 6, the tsunami inundations at
162 Puerto Cortes computed from those two initial conditions are compared. The tsunami numerical
163 simulations from both initial conditions cause limited inundations and do not cause serious
164 damages in the port area although the tsunami heights from the tsunami initial condition with the
165 effect of the horizonal displacement are larger than those from the tsunami initial condition
166 without the effect.

167 In Figure 7, the tsunami initial conditions from the small fault model with the effect of the
168 horizontal displacement and without that are compared. In Figure 8, the tsunami inundations at
169 Puerto Cortes computed from those two initial conditions are compared. The western part of the
170 beach and city are inundated by tsunamis of about 4 m maximum height from both initial
171 conditions. The port area is also inundated by the tsunami. The inundation area computed from
172 the initial condition with the effect of the horizontal displacement is slightly larger than that from
173 the initial condition without that. Especially, at the port area, shown as a red ellipse in Figure 8,
174 the tsunami inundation is larger for the tsunami initial condition with the horizontal displacement
175 effect than that for the initial condition without the effect. Figure 9 shows the comparison of two
176 computed tsunami waveforms with and without the effect of horizonal displacement. The
177 maximum tsunami height from the initial condition with the horizontal displacement effect is
178 14 % larger than that from the initial condition without the effect.
179

180 ## 5. Discussions

181 Because the 2018 large Swan Island earthquake (Mw 7.6) occurred far from the coast of Central

America (Figure 1), only small tsunami, less than 20 cm, was observed. The results in this study show that the same size of earthquake occurred near Puerto Cortes along the left-lateral Swan Island Fault zone cause significant tsunami inundation which could damage one of the largest ports in Central America and the residents. Large cargo boats in the port can be damaged easily by those tsunamis. Large cargo boats carried by the tsunamis also damage the port and residents. It is important to understand this possible tsunami hazard and prepare for that.

The horizontal displacement of ocean bottom slops near the Swan Island Fault zone in this area enhanced the tsunami generation as shown in Figure 7. In general, strike-slip type earthquakes cause much larger horizontal displacement than vertical displacement. This causes that the enhancement of tsunami generation due to the horizontal displacement of the ocean slops by strike-slip type earthquakes is more significant than that the enhancement by the dip-slip earthquakes. Figure 9 indicates that the enhancement in this study reaches about 14% of the tsunami height without the horizontal displacement effect.

6. Conclusions

The tsunami inundation at Puerto Cortes was computed from two fault models in the Swan Island Fault zone, the long fault model estimated from the scaling relationships (Blaser et al., 2010) and the small fault model estimated from the slip distribution based on the 2018 Swan Island earthquake. The tsunami computed from the small fault model with a large slip amount of 20.8 m inundated a large area of Puerto Cortes including the important port area. Large cargo boats in the port can be damaged easily by those tsunamis. The effect of the co-seismic horizontal displacement of the ocean floor also enhanced the tsunami inundation at Puerto Cortes.

The Swan Island Fault zone accommodates the relative motion between the North American and Caribbean plates, 2 cm/yr (Dixon et al., 1998, ten Brink et al, 2002, Mann, 2007). Consequently, the large earthquakes repeatedly occurred along the Swan Island fault zone, such as the 1976

Guatemala earthquake (Ms 7.5), the 1999 Guatemala earthquake (Mw6.7), the 2009 Off Honduras earthquake (Mw 7.3), and the 2018 Swan Island earthquake (Mw 7.6). However, no large earthquake (Ms > 7) occurred off Puerto Cortes along the fault zone at least 50 years. We need to prepare for a large future earthquake off Puerto Cortes and tsunami hazard at Puerto Cortes.

Acknowledgments

We thank two anonymous reviewers and an editor for useful comments to improve the manuscript. This study is supported by the JICA Project for Strengthening of Capacity of the Central American Tsunami Advisory Center (CATAC).

References

Blaser, L., Kru¨ger, F., Ohrnberger, M., and Scherbaum, F., (2010). Scaling relations of earthquake source parameter estimates with special focus on subduction environment. Bulletin of the Seismological Society of America, 100(6), 2914–2926. doi:10.1785/0120100111.

Dixon, T. H., Farina, F., DeMets, C., Jansma, P. E., Mann, P., and Calais, E. (1998). Relative motion between the Caribbean and North American plates and related boundary zone deformation from a decade of GPS observations. Journal of Geophysical Research, 103, 15157–15182.

Duputel, Z., Rivera, L., Kanamori, H., and Hayes, G. (2011). Realtime W phase inversion during the 2011 off the Pacific coast of Tohoku earthquake. Earth Planets Space, 63, 535–539. doi:10.5047/eps.2011.05.032.

Fritz, H.M., J.V. Hillaire, E. Molière, Y. Wei, and F. Mohammed (2013). Twin tsunamis triggered by the 12 January 2010 Haiti earthquake. Pure Appl. Geophys., 170(9-10):1463-1474, doi:10.1007/s00024-012-0479-3.

Goto, C., Ogawa, Y., Shuto, N., and Imamura, F., (1997). IUGG/IOC time project: Numerical

method of tsunami simulation with the leap-flog scheme, IOC of UNESCO, manuals and guides 35.

Imamura, F. (1996). Review of tsunami simulation with a finite difference method. In H. Yeh, P. Liu, and C. Synolakis (Eds.), Long-Wave Runup Models (pp. 25–42). World Scientific.

Kanamori, H., & Rivera, L. (2008). Source inversion of W phase: speeding up seismic tsunami warning. Geophysical Journal International, 175(1), 222–238.

Mann, P., (2007), Overview of the tectonic history of northern Central America, *in* Mann, P., ed., Geologic and tectonic development of the Caribbean plate boundary in northern Central America: Geological Society of America Special Paper 428, 1–19, doi:10.1130/2007.2428(01).

Okada, Y., (1985), Surface deformation due to shear and tensile faults in a half-space. Bulletin of the Seismological Society of America, 75, 1135–1154.

Plafker, G., (1977), Color slides showing geologic effects and damage caused by the destructive Guatemala earthquake of February 4, 1976, United State Department of the Interior, Geological Survey Open-file Report 77-165, 1-10.

Strauch, W., Talavera E., Tenorio V., Ramirez J., Arguello G., Herrera M., Acosta A., and Morales A., (2018), Toward an Earthquake and Tsunami Monitoring and Early Warning System for Nicaragua and Central America, Seismological Research Letters, 89, 400-406, doi: 10.1785/0220170193.

Tanioka, Y., and Satake, K. (1996), Tsunami generation by horizontal displacement of ocean bottom. Geophysical Research Letters, 23(8), 861-864

ten Brink, U.S., Coleman, D.F., and Dillon, W.P. (2002), The nature of the crust under Cayman trough from gravity: Marine and Petroleum Geology, 19, 971–987, doi: 10.1016/S0264-8172(02)00132-0.

Figure Captions

Figure 1. Large earthquakes occurred along the Swan Island Fault Zone, the 1976 Guatemala earthquake (Ms7.5), the 1999 Guatemala earthquake (Mw 6.7), the 2009 Off-Honduras earthquake (Mw7.3), and the 2018 Swan Inland earthquake (Mw7.6). The red line shows the Swan Island Fault Zone (after ten Brink et al., 2002).

Figure 2. Four nested grid systems (R1, R2, R3, and R4) for the tsunami numerical simulation. Tsunami inundation simulation is carried out for R4 region at Puerto Cortes. The red line shows the Swan Island Fault Zone (after ten Brink et al., 2002).

Figure 3. Bathymetry and topography in R4 region (Puerto Cortes) where tsunami inundation simulation is carried out.

Figure 4. The focal mechanism and fault model (a black rectangular) of the 2018 Swan Island earthquake estimated using the W-phase inversion and the scaling relationships between magnitude and the fault length or width (Blaser et al., 2010). Purple rectangles show two fault models, 136 km x 24 km, and 40 km, x 20 km, for the tsunami hazard evaluation at Puerto Cortes. The red line shows the Swan Island Fault Zone (after ten Brink et al., 2002).

Figure 5. Tsunami initial sea surface deformation for the long fault model (136 km x 24 km) from the scaling relationships (Blaser at al., 2010). a) no effect of the co-seismic horizontal displacement. b) including the effect of the co-seismic horizontal displacement.

Figure 6. The results of the tsunami inundation at Puerto Cortes computed from the initial sea surface deformation in Figure 5 using the long fault model. a) no effect of the co-seismic horizontal displacement. b) including the effect of the co-seismic horizontal displacement.

286

287 Figure 7. Tsunami initial sea surface deformation for the small fault model (40 km x 20 km) based
288 on the slip distribution estimated by the USGS. a) no effect of the co-seismic horizontal
289 displacement. b) including the effect of the co-seismic horizontal displacement.

290

291 Figure 8. The results of the tsunami inundation at Puerto Cortes computed from the initial sea
292 surface deformation in Figure 7 using the small fault model. a) no effect of the co-seismic
293 horizontal displacement. b) including the effect of the co-seismic horizontal displacement. Red
294 ellipse shows the port area. A black dot shows a location of tsunami waveform comparison in
295 Figure 9.

296

297 Figure 9. Comparison of tsunami waveforms at a position, P, in Figure 8 for the initial condition
298 with horizontal displacement effect (blue) and for that without the effect (red).

299

300

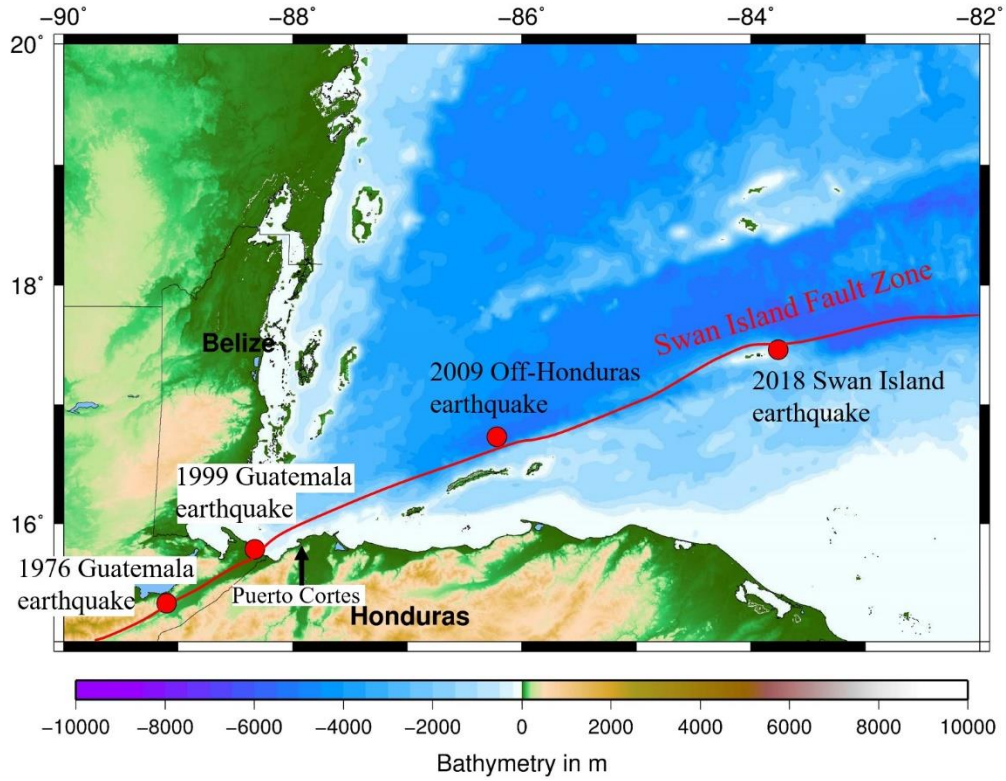

Figure 1.

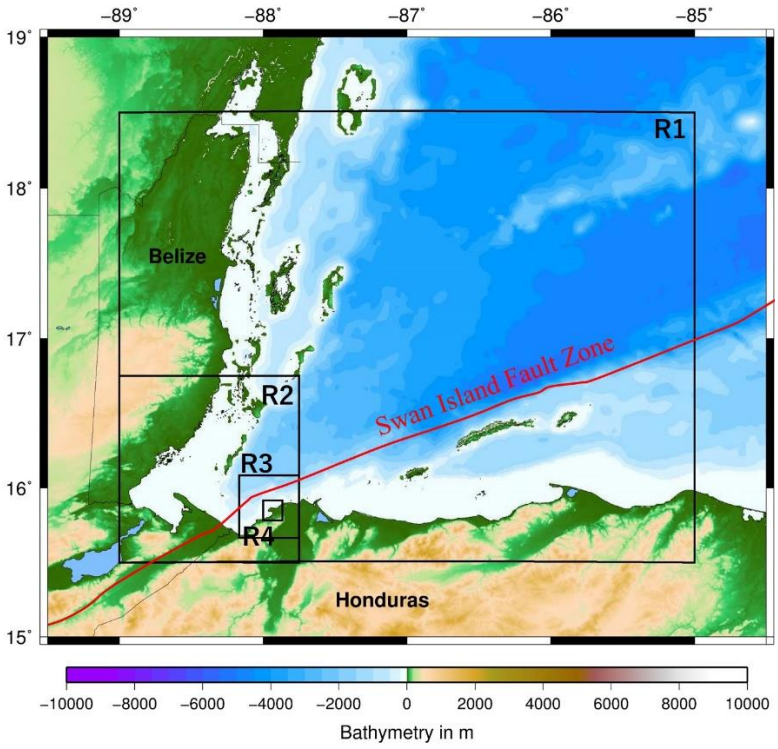

Figure 2.

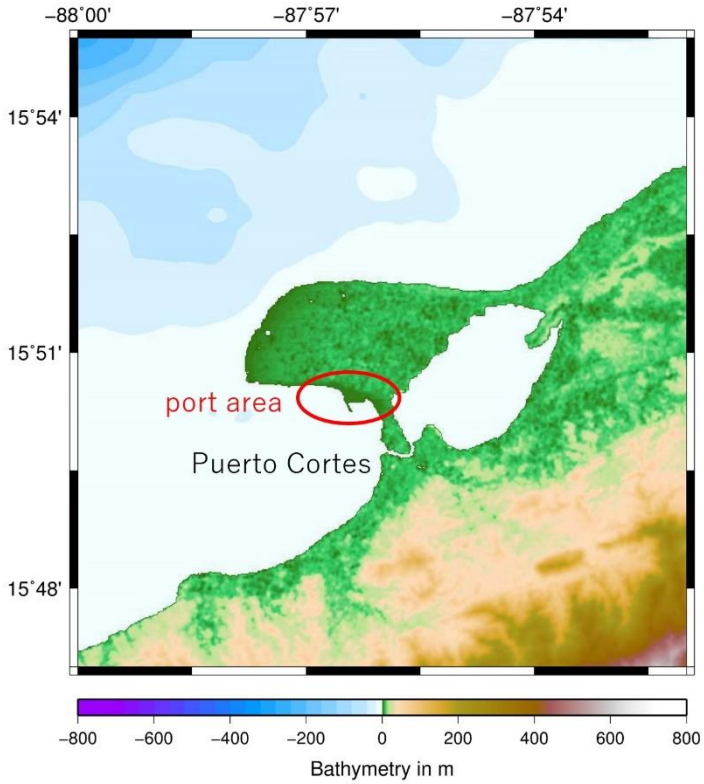

Figure 3.

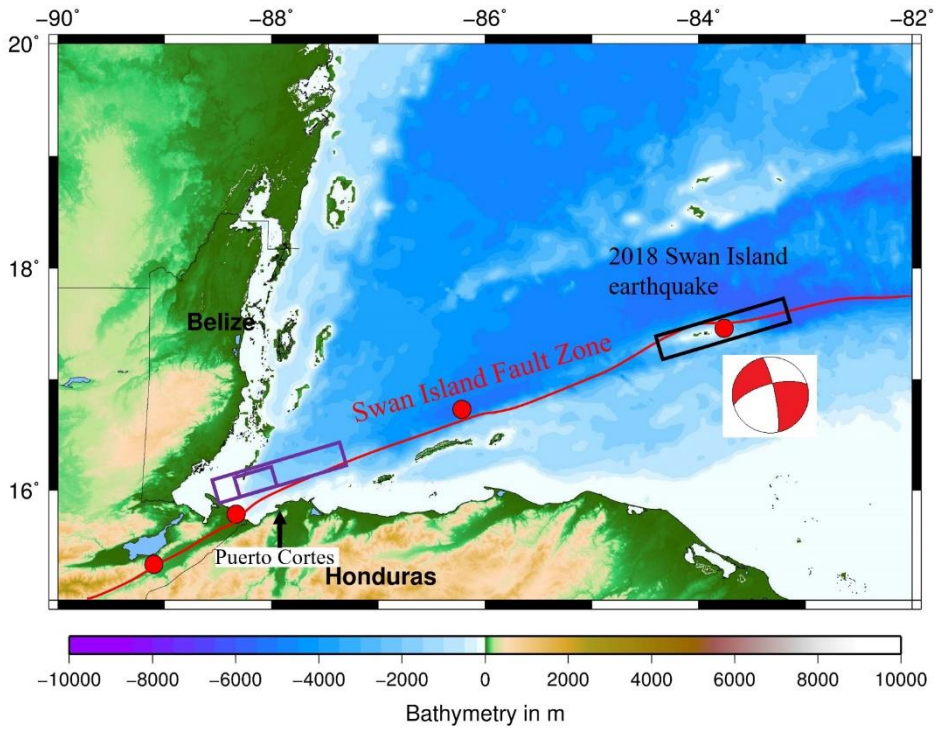

Figure 4.

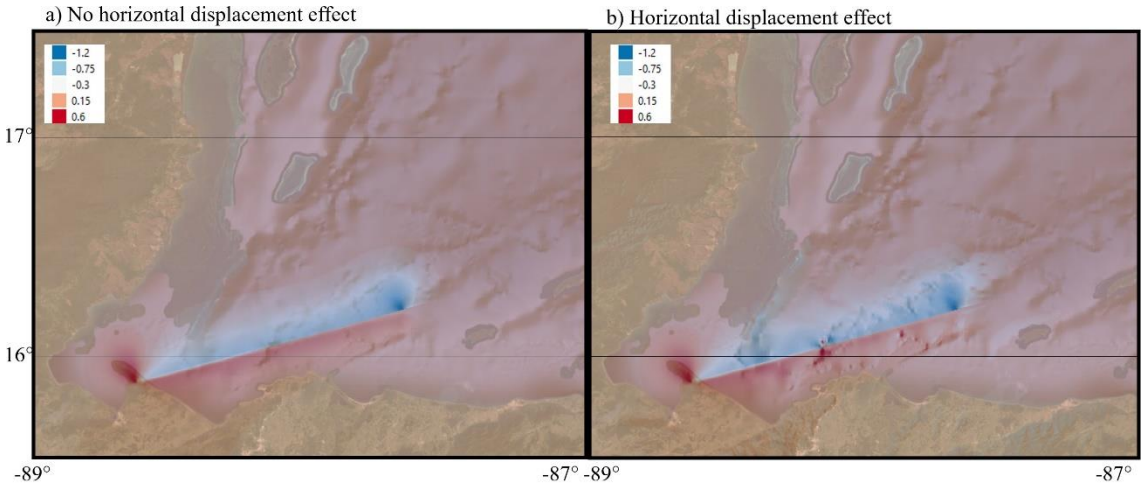

311

312 Figure 5.

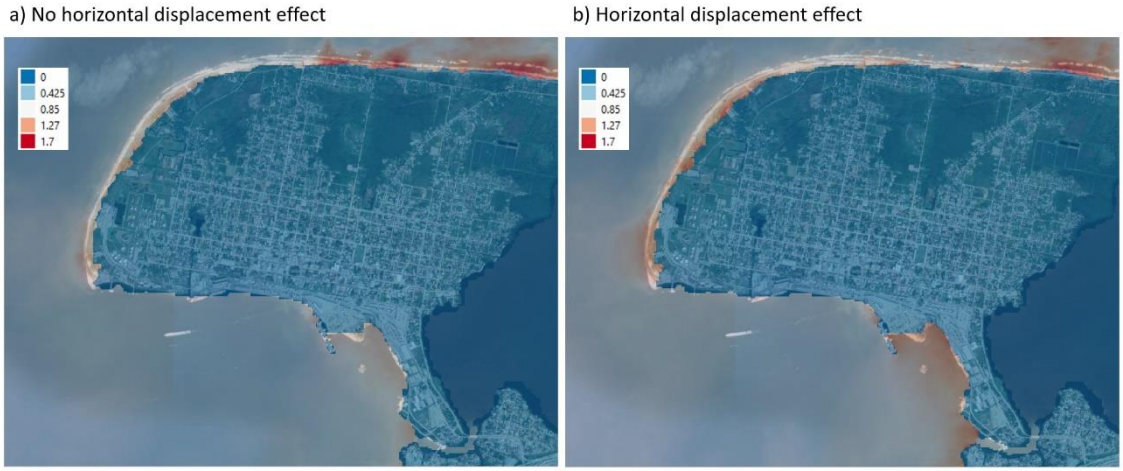

313

314 Figure 6.

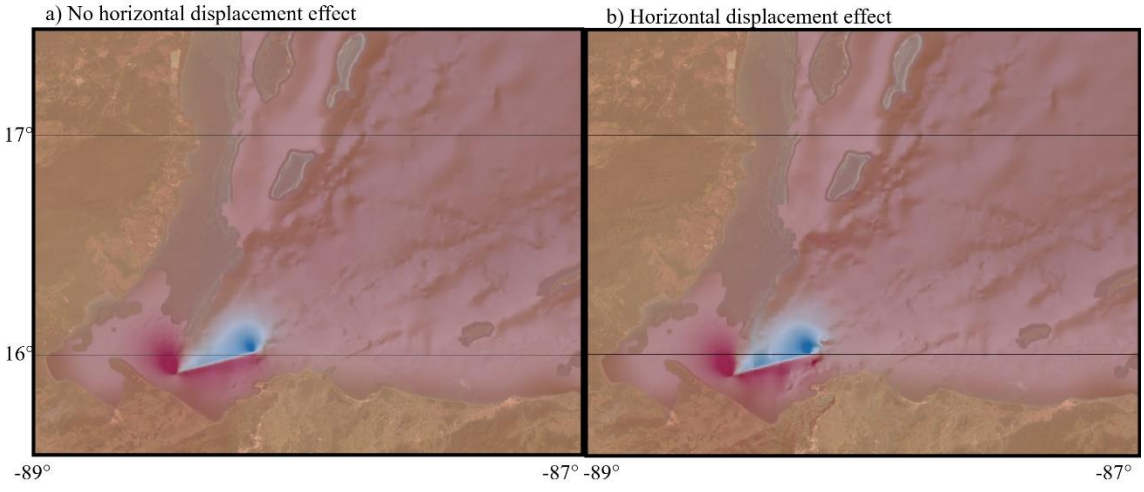

315

316 Figure 7.

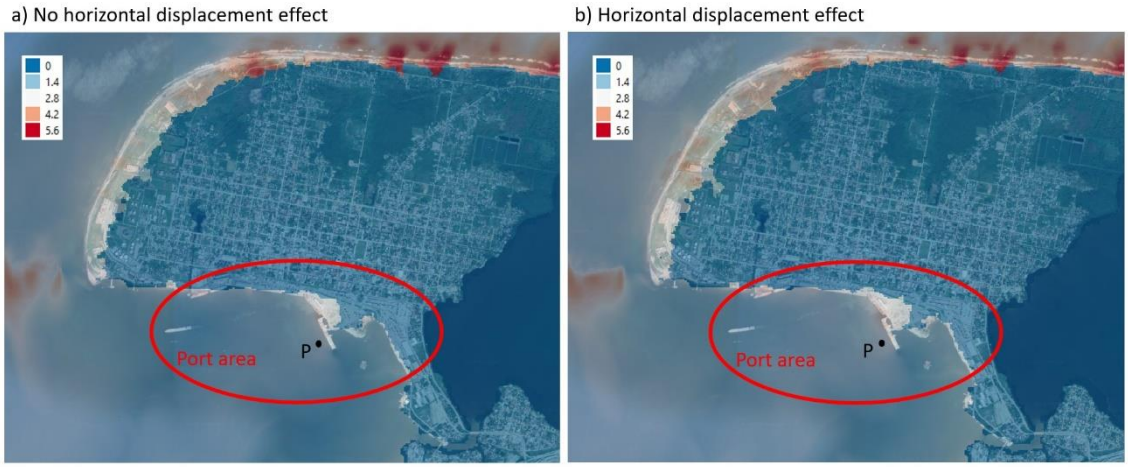

317

318 Figure 8.

319

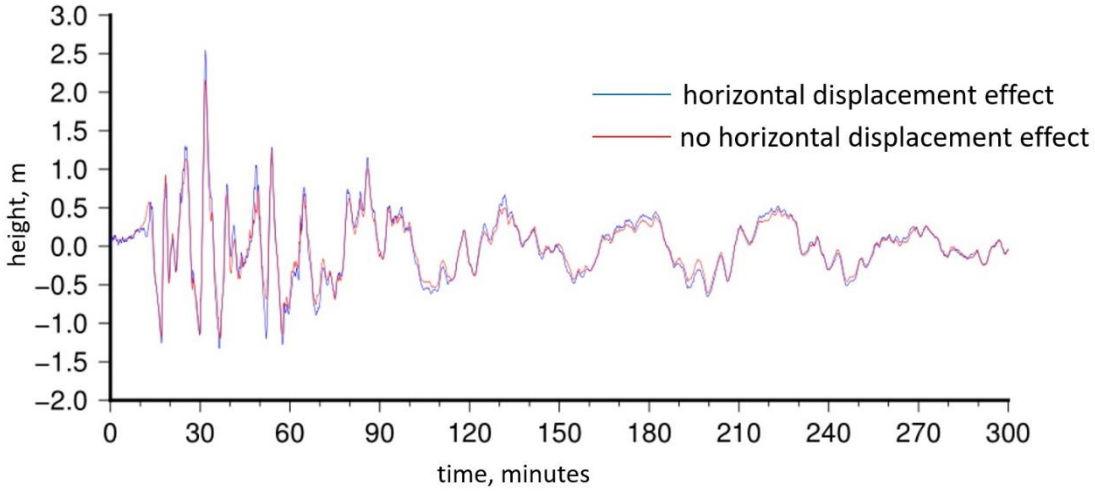

320

321 Figure 9